Attractions in Sterically Stabilized Silica Dispersions

III. Second Virial Coefficient as a Function of Temperature, as Measured by Means of Turbidity

J. W. JANSEN, C. G. DE KRUIF, AND A. VRIJ

Van't Hoff Laboratory for Physical and Colloid Chemistry, University of Utrecht, Padualaan 8, 3584 CH Utrecht, The Netherlands

Received September 2, 1985; accepted January 28, 1986

Silica particles coated with octadecyl chains and dispersed in toluene exhibit attractions on lowering the temperature. The attraction is supposed to be the result of interactions between the chain segments and solvent. Since light is strongly scattered in the dispersions turbidity measurements are used to study the interactions. It is shown that turbidity (extrapolated to infinite wavelength) gives the same information as angular light scattering, provided the particles are small. A square well potential with a narrow width and a temperature-dependent depth describes quite well the measured second viral coefficients. In addition the refractive index of the particles as a function of wavelength is also obtained.

1. INTRODUCTION

In our laboratory we have constructed a colloidal system that consists of spherical silica particles densely covered with linear hydrocarbon chains which are attached terminally to the particle surface (1). These chains, 18 C atoms long, provide the steric stabilization when the particles are dispersed in a solvent. They also prevent the formation of siloxane bridges between the particles on drying. In a solvent-like cyclohexane the particle interactions can be described with the so-called hard sphere model (2). In other solvents, as was shown in previous papers, the particles may exhibit attractions when the temperature is lowered, eventually leading to phase separation (3, 4). These attractions are connected with the quality of the solvent with regard to the stabilizing chains. For instance cyclohexane is a good solvent in which attractions are not noticeable, whereas ethanol is a bad solvent with strong attractions. The London–van der Waals attraction between the particle cores plays a minor role, because the particles are small and the refractive indexes of particle core and solvents differ only slightly (3). Quantitative calculations of these forces sustain this conclusion.

With light scattering techniques (both static and dynamic) much information can be obtained from colloidal systems. At low particle concentrations the molar mass and size of the particles can be determined. At higher concentrations the interactions between the scattering species become more important and can be studied. In this paper we report on measurements done on colloidal silica systems where turbidity was used as a probe to investigate the interactions. In principle the same information can be obtained from turbidity as from light scattering, provided the particles are small (diameter < 100 nm). A description will be given of the procedure by which this information is obtained by an extrapolation to wavelength infinity, which is the equivalent of extrapolation to wave vector zero in angular light scattering experiments.

Conventional light scattering methods cannot be used with the systems we constructed since the samples scatter so much light that multiple scattering becomes disturbing and

0021-9797/86 $3.00

prevents an unambiguous interpretation (even with a recently developed correction procedure for double scattering (5)). It appears, however, that turbidity measurements on our dispersions are affected only negligibly by multiple scattering and can therefore be used to study interactions. This will be discussed in Section 3.3 and illustrated in experiments.

Turbidity measurements were done on a colloidal system (code SJ9). This system was also used in phase separation experiments (4).

2. THEORY

Turbidity is the attenuation of a light beam by scattering when it passes through a sample. It is defined as $\tau = l^{-1} \ln(I_t/I_0)$ where I_0 is the incident intensity, I_t is the transmitted intensity, and l the length of the light path in the sample. When adsorption is excluded the amount of light must be conserved: $I_0 = I_t + \sum I_s$. Here $\sum I_s$ is the intensity of light scattered in all directions. The relative scattered intensity or Rayleigh ratio $R(K)$ is defined by $R(K) = I_s r^2/I_0 V_s$ (where r is the distance from sample to detector and V_s the volume of the illuminated part "seen" by the detector) and under certain conditions is equal to

$$R(K) = K^* cMP(K)S(K)(1+\cos^2\theta)$$

$$K^* = \frac{2\pi^2 n^2 (dn/dc)^2}{\lambda_0^4 N_A}. \qquad [1]$$

Here n is the refractive index of the sample, N_A Avogadro's number, λ_0 the wavelength in vacuum, c the weight concentration, and M the molar mass of the particles. The form factor $P(K)$ accounts for the interference of light scattered from various parts of one particle and the structure factor $S(K)$ for the interference between various particles in the sample. The wave vector K is equal to $4\pi n/\lambda_0 \sin(\theta/2)$ with θ the angle between scattered and transmitted light. The structure factor $S(K)$ contains information about the interaction. Equation [1] is based on the Rayleigh–Gans–Debye (RGD) theory of light scattering which applies when $d(n_p - n_0) < \lambda_0/10$, where d is the diameter of the particles. This equation describes single scattering only. The relation between turbidity and scattered intensity is

$$\tau = 2\pi \int_0^\pi R(K) \sin\theta \, d\theta. \qquad [2]$$

For very small particles (radius < 10 nm) $R(K)$ is proportional to $1 + \cos^2\theta$ and the integration is easily performed, leading to the well-known result: $\tau = (16/3)\pi R$ ($\theta = 90°$) $= (8/3)\pi R$ ($\theta = 0°$). In this situation turbidity contains the same information as scattered intensity.

The K dependence of the structure factor $S(K)$ can be neglected for small particles and is equal to $S(K = 0)$. $S(K = 0)^{-1}$ is proportional to the osmotic compressibility which is written in a virial expansion

$$S(K=0)^{-1} = 1 + 2B_2 c + 3B_3 c^2. \qquad [3]$$

The second virial coefficient B_2 is related to the potential of mean force which at low concentration is equal to the interaction potential $V(r)$:

$$B_2 = \frac{N_A}{M} 2\pi \int_0^\infty (1 - e^{-V(r)/kT}) r^2 dr. \qquad [4]$$

From B_2 information on the interaction can be obtained by plotting c/τ versus c. At low particle concentration the initial slope of this plot divided by the intercept equals $2B_2$. The molar mass of the particles is obtained from the intercept which is equal to $(16/3\pi MK^*)^{-1}$.

For our particles the interaction potential is modeled as a repulsive hard sphere to which an attractive square well potential is added (3):

$$\begin{aligned} V(r) = \infty \quad & r < \sigma \\ -\epsilon \quad & \sigma < r < \sigma + \Delta \\ 0 \quad & r > \sigma + \Delta. \end{aligned}$$

We assume that the depth of the well, ϵ, depends on temperature:

$$\begin{aligned} \epsilon &= L\left(\frac{\theta}{T} - 1\right) kT; \quad T \leqslant \theta \\ \epsilon &= 0; \qquad\qquad T > \theta. \end{aligned} \qquad [5]$$

θ Is the theta temperature of the stabilizing chain–solvent pair. The factor L is proportional to the volume of overlap of the chains

and thus depends on the size of the particles. With this interaction potential B_2 is found to be

$$B_2 = q\left\{4 + 12\frac{\Delta}{\sigma}(1 - e^{L[(\theta/T)-1]})\right\} \quad [6]$$

where $q = (1/6)\pi\sigma^3 N_A/M$, a specific volume of interaction. Note that the first term, $4q$, is due to the hard sphere interaction and the second term due to the attractive well. In formulating Eq. [6] we assumed that $\Delta \ll \sigma$. This seems appropriate because in our particles the hydrocarbon layer is thin with respect to the diameter of the core.

For larger particles (or shorter wavelengths) the dependence of $R(K)$ on K must be taken into account. For not too large particles (radius <50 nm) this is taken into account by expressing $P(K)$ as $1 - K^2R_g^2/3$, where R_g is the optical radius of gyration of the particles. $S(K)$ is given by

$$S(K) = 1 + 4\pi\rho\int_0^\infty (g(r) - 1)\frac{\sin Kr}{Kr}r^2 dr \quad [7]$$

where ρ is the (number) concentration and $g(r)$ the radial distribution function, which for low concentrations is equal to $\exp(-V(r)/kT)$. Expanding Eq. [7] in terms of K^2 we find, up to terms linear in the particle concentration

$$S(K) = 1 - \phi(8 - \alpha) + \phi\frac{K^2\sigma^2}{10}\left(8 - \frac{5}{3}\alpha\right) \quad [8]$$

where $\alpha = 24(\Delta/\sigma)(e^{L[(\theta/T)-1]} - 1)$ and ϕ is $(1/6)\pi\sigma^3\rho$, the hard sphere volume fraction. Note that $\phi = qc$.

The form of Eq. [8] is retained when the shape of the attractive well is not square, as long as the range of the well is small compared to the particle size. In that case it is easy to show that

$$\alpha = \frac{24}{\sigma}\int_\sigma^\infty (e^{-V(r)/kT} - 1)dr \quad [9]$$

where $V(r)$ is the attractive well potential.

Having expressed both $P(K)$ and $S(K)$ as a function of K we perform the integration of Eq. [2] and the turbidity is found to be

$$\tau = K^* cM\frac{16}{3}\pi\left\{1 - \frac{8}{3}\left(\frac{4\pi n}{\lambda_0}\right)R_g^2\right\}$$
$$\times\left\{1 - \phi(8 - \alpha) + \phi\frac{4}{5}\left(8 - \frac{5}{3}\alpha\right)\left(\frac{\pi n\sigma}{\lambda_0}\right)^2\right\}. \quad [10]$$

By plotting c/τ versus c and determining the slope, we obtain an apparent second virial coefficient, which is equal to

$$B_{2,\mathrm{app}}(\lambda_0) = q\left\{4 - \frac{\alpha}{2} - \frac{4}{5}\left(4 - \frac{5}{6}\alpha\right)\left(\frac{\pi n\sigma}{\lambda_0}\right)^2\right\}. \quad [11]$$

The limiting value of B_2 ($K \to 0$) (see Eq. [6]) can be found by plotting $B_{2,\mathrm{app}}(\lambda_0)$ versus λ_0^{-2} and extrapolating to $\lambda_0^{-2} = 0$.

The molar mass M cannot be calculated readily from the intercept of c/τ versus c, because K^* depends on λ_0 via the term λ_0^4, but also via the refractive index and the refractive index increment dn/dc. Usually this last quantity is not known accurately enough as a function of λ_0 in order to perform a reliable extrapolation.

Of course turbidity changes when the contrast, i.e., the difference between refractive index of particle and solvent, is changed. Using mixtures of solvents this contract can easily be varied. The turbidity at low concentrations as a function of refractive index is described by

$$\frac{\sqrt{\tau}}{n_0} = (n_p - n_0)$$
$$\times\left\{\frac{2\pi^2}{\delta^2 N_A\lambda_0^4}cM\frac{16}{3}\pi\left(1 - \frac{8}{3}\left(\frac{4\pi n}{\lambda_0}R_g\right)^2\right)\right\}^{1/2}. \quad [12]$$

This equation is derived using $dn/dc = (n_p - n_0)/\delta$ where δ is the particle specific mass. A plot of $\sqrt{\tau}/n_0$ versus n_0 thus gives two straight lines which intersect the n_0-axis at the so-called matchpoint. A single line may be obtained when one of the branches is reflected in the n_0 axis. The slope of this line is proportional to M, while the matchpoint gives the mean refractive index of the particles.

3. EXPERIMENTAL

3.1. Materials and Method

The following chemicals were used to synthesize the silica particles: ethanol 100% technical grade, distilled before use; concentrated ammonia (Merck); tetraethoxysilane (TES) (Fluka), vacuum distilled before use; and octadecyl alcohol 98% (Merck). The solvents *n*-hexane, toluene (Baker), and *p*-xylene (Fluka) were used as received.

Turbidity is measured with a Shimadzu (Spectronic 200 UV) double beam spectrophotometer and glass cuvettes (Hellma). The cuvette holder is thermostated by a flow of water from a water bath. Temperature is measured in this water bath and corrected for the (calibrated) temperature difference between bath and cuvette. Temperature equilibrium is believed to be reached when the transmission of the sample becomes constant. The turbidity is obtained by measuring the transmission of a cuvette filled with pure solvent and of the same cuvette filled with sample: $\tau = l^{-1} \ln(I(\text{sample})/I(\text{solvent}))$. Consequently there was no need to use matched cuvettes.

The inaccuracy in the transmission values is about 0.003 depending on wavelength. Therefore the turbidities measured on samples with a transmission >0.95 or <0.03 become rather inaccurate.

3.2. Synthesis and Characterization

The silica system is synthesized according to van Helden *et al.* (1) and coded SJ9. The concentrations of TES, ammonia, and water used were 0.17, 0.68, and 1.65 *M*, respectively. The particles are coated with octadecyl alcohol by an esterification reaction of the alcohol with the surface silanol groups. The silica is purified by distilling off the excess alcohol and repeated ultracentrifugation, the supernatant being discarded.

Elemental analysis showed that the weight percentage of organic material (calculated as $C_{18}H_{37}O_{0.5}$) is 11.7. The size of the particles was measured with transmission electron microscopy and the mean radius was found to be 31 nm and the width of the distribution was 4 nm. The radius measured with photon correlation spectroscopy (PCS) is 37 nm. (The difference between these two radii is discussed in Ref. (1).) The density of the particles is 1.75 $\pm$ 0.02 g/cm^3 and was found from the pycnometric density of a dispersion of known concentration.

3.3. Turbidity Measurements

In the derivation of Eq. [2] it is assumed that scattered light does not reach the detector. However, in an experimental setup this can occur in two ways. First, light scattered at very small angles can be detected together with the transmitted beam. Walstra (7) found that for small particles the angle subtended by the detector may be up to 9° before scattered light becomes disturbing. We checked this by using a slit of 1-mm width at a distance of about 4 cm from the cuvette. This slit was just a little wider than the width of the undisturbed light beam, i.e., obtained when a cuvette filled with solvent was placed in the holder. The slit has an aperture of 2°, which was adequate. We did not find a change in turbidity even for the highest turbidities, therefore we conclude that little or no scattered light reaches the detector. For larger particles, where much light is scattered in the forward direction, the angle of subtention must be smaller. For large particles ($a > 300$ nm) this condition becomes difficult to fulfill, but then Eq. [8] may not be used either. Second, spurious reflections of inadequate equipment can reach the detector. The effect will be slight as the side walls of the cuvette are relatively far away from the light beam. Furthermore reflections are negligible since the refractive indexes of the solvents used are about equal to the refractive index of glass.

4. RESULTS

4.1. Contrast Variation

We did two tests to check whether multiple scattering influenced the measured turbidities.

(1) We measured the turbidity of a sample of SJ9 in toluene at various wavelengths and in three cuvettes each with a different length of the light path. Results are given in Table I. It can be seen that within experimental error τ does not depend on cuvette length.

(2) A contrast variation experiment was performed. The turbidity (at 25°C) was measured of dispersions of SJ9 (c = 0.014 g/cm^3) in mixtures of n-hexane and toluene. These dispersions were made by mixing dispersions of equal concentration in both pure solvents. The refractive indexes of the mixtures at λ_0 = 436, 546, and 578 nm were measured with a Pulfrich refractometer and from these indexes we calculated the indexes for the wavelengths used in the spectrophotometer (using a linear dependence of n on λ_0^{-2}). In Fig. 1 some results are shown for a few wavelengths in the way described in Section 2. It is found that the experimental points lie on a straight line even for the highest turbidities (τ_{max} = 4 cm^{-1}). We therefore conclude that multiple scattering has only a slight effect (if any) on the turbidities measured. In static light scattering experiments multiple scattering becomes disturbing at turbidities of 0.1 cm^{-1} (5).

The difference in the significance of multiple scattering for angular scattering and for turbidity experiments can be understood if one realizes that multiple scattering changes the angular distribution of the scattered intensity. It has however no influence on the total amount scattered over all angles. Stated differently: in turbidity experiments it does not matter if light scattered once and thus taken

TABLE I

Variation of τ with Cuvette Length

λ_0 (nm)	l/mm 1	5	10
400	9.18 ± 0.08	8.9 ± 0.4	—
600	1.17 ± 0.05	1.206 ± 0.012	1.224 ± 0.01
800	0.30 ± 0.05	0.345 ± 0.015	0.35 ± 0.01

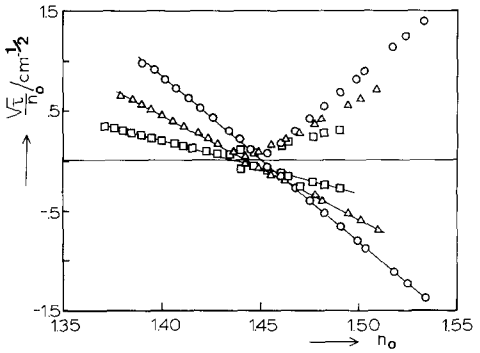

FIG. 1. The square root of the turbidity is plotted against the refractive index of the solvent mixture (n-hexane/toluene); ○, λ_0 = 350 nm; △, λ_0= 450 nm; and □, λ_0 = 550 nm.

away from the ongoing beam is scattered again (as long as it does not reach the detector finally). Thus when multiple scattering is present the use of Eq. [1] in the combination of Eq. [2] remains valid. The use of Eq. [1] is restricted to the RGD domain and to cases where the reciprocal τ is much larger than the range of the radial distribution function $g(r)$.

The contrast variation technique gives the refractive index of the particles as a function of wavelength. This is plotted in Fig. 2 against λ_0. Also from the refractive index increment and the density of the particles one can calculate the refractive index of the particles. We measured dn/dc and found it to be 0.0352 ± 0.0004 cm^3/g (λ_0 = 546 nm) and 0.0405 ± 0.0006 cm^3/g (λ_0 = 436 nm). The calculated

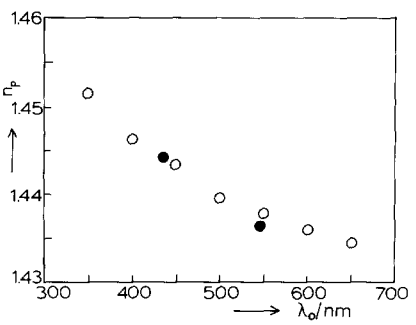

FIG. 2. The refractive index of the particles is plotted against wavelength. ○, Found with turbidimetry. ●, Found from dn/dc.

n_p's (1.4364 for λ_0 = 546 and 1.4442 for λ_0 = 436 nm) are plotted in Fig. 2 also. Both techniques result in the same n_p. These results can be used to obtain the absorption frequency of the silica particles, which is required for the calculation of the Hamaker constant (3). Plotting $(n_p^2 + 2)/(n_p^2 - 1)$ (i.e., proportional to the polarizability) (8) versus ν^2 ($=c^2\lambda_0^{-2}$; where c is the velocity of light) results in Fig. 3. The absorption frequency is then $39.2 \pm 0.3\ 10^{14}$ s^{-1}, which complies with the literature value that we used for fused silica in Ref. (3).

From the slopes of the plots in Fig. 1, from the measured density, and by extrapolating to wavelength infinity we found (Eq. [12]) that $M = (2.4 \pm 0.2)\ 10^8$ g · mole^{-1}. Concentration ($c = 0.014$ g · cm^{-3}) is considered low enough for $S(K)$ to be 1. From M and the density a radius of 38 ± 1 nm is calculated which is equal to that found with PCS.

4.2. *Virial Coefficients*

The turbidity of dispersions of silica in toluene and in *p*-xylene in a concentration range of 0.01–0.2 g · cm^{-3} was measured. In order to make the necessary extrapolation to wavelength infinity we measured at wavelengths ranging from 400 nm to 800 nm. For each solvent we also varied the temperature, which in turn altered the interaction. As an example some of the results for the silica in toluene are plotted in Figs. 4 and 5. The effect of the temperature is clearly seen from the varying slope in Fig. 4. The intercept of the (least squares) fitted straight lines changes also, because the contrast changes with temperature. Figure 5 shows the effect of the variation of wavelength. The apparent second virial coefficient is obtained by dividing the slope by the intercept. In Fig. 6 this $B_{2,app}$ is plotted versus λ_0^{-2} and the extrapolation to $\lambda_0^{-2} = 0$ is shown.

For toluene the B_2 values at two wavelengths and extrapolated to $\lambda_0^{-2} = 0$ are plotted in Fig. 7 as a function of temperature. For *p*-xylene only the extrapolated values are shown. The drawn line in Fig. 7 is a theoretical fit made

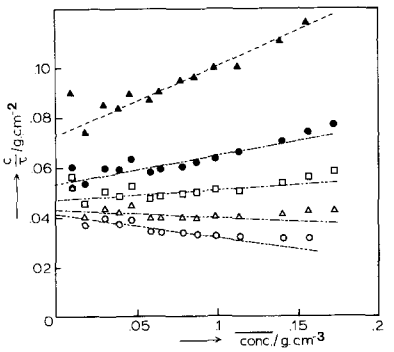

FIG. 4. c/τ Is plotted against concentration c of the silica particles dispersed in toluene for various temperatures. ○, T = 11.1; △, T = 13.4; □, T = 18.0; ●, T = 24.4, and ▲, T = 39.6°C. Turbidities were measured at λ_0 = 600 nm.

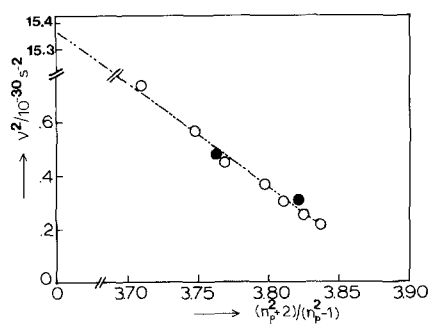

FIG. 3. A plot of the squared frequency against $(n_p^2 + 2)/(n_p^2 - 1)$ for estimation of the adsorption frequency of silica particles by extrapolating to $(n_p^2 + 2)/(n_p^2 - 1) = 0$.

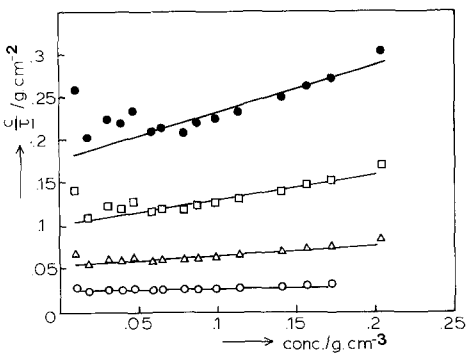

FIG. 5. c/τ Is plotted against concentration c of the silica particles dispersed in toluene for various wavelengths, ○, λ_0 = 500 nm; △, λ_0 = 600 nm; □, λ_0 = 700 nm; and ●, λ_0 = 800 nm. Temperature was 24.4°C.

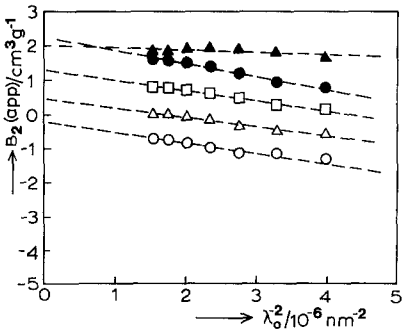

FIG. 6. The apparent second viral coefficient as a function of λ_0^{-2} at various temperatures. For symbols see Fig. 4. The extrapolation to $\lambda_0^{-2} = 0$ is shown.

with Eq. [6] where we used $q = 0.8$ cm$^3 \cdot$ g^{-1}, $\sigma = 70$ nm. Taking $\Delta = 0.1$ nm it is found that L is 22.8 and θ is 353 K. More or less the same curve will be found using $\Delta = 0.2$ nm and $L = 23.2$ and $\theta = 345$ K.

5. DISCUSSION

The particle interaction in toluene is clearly dependent on temperature as can be seen from Fig. 4 or in more detail from Fig. 7. For the results at high temperatures the slopes of c/τ versus c in Fig. 4 are positive as they should be when the interactions are repulsive. In *p*-xylene the slopes are positive too (not shown). At lower temperatures the slope and thus B_2 decreases, indicating that an attraction is developing in the interaction potential (cf. Eq. [4]). The Boyle temperature, i.e., where B_2 equals zero is found at 12°C. At this temperature B_2 very quickly becomes more negative and will become low enough to induce a separation into two phases; this occurs at about 9.5°C (4).

The variation of B_2 with temperature is also found for gases (9), polymer solutions, and microemulsions (10, 11). The mechanism responsible for the interaction is the London–van der Waals attraction, which favors condensation and is counterbalanced by the entropy, which in turn favors evaporation or dilution. Together they determine the free energy. The interaction will depend on temperature and, except in the case of gases, on solvent. The number of contacts between the interacting species determine the temperature range in which the interaction changes from pure repulsive to attractive, eventually leading to phase separation. For our particles and for microemulsions (10) the particles interact through the chains on the surface. For short chains the number of contacts will be smaller than for polymers (or polymer coated particles), but of course much larger than for gases. This results in a temperature range smaller than that of gases (where it is hundreds of degrees) and larger than that of high molecular weight polymers (a fraction of a degree) (12). The range of attraction will be about 0.1 nm, since the chains on the particles are densely packed and can hardly interpenetrate. We have proposed an interaction potential where the attraction is described with a polymer-like theory. The depth of the attractive well is inversely correlated with the chosen width (Eq. [6]) and is plotted as a function of temperature in Fig. 8. One can see that the attractive potential reaches a few kT.

The particles in *p*-xylene do not show a variation of B_2 with temperature. Evidently there is no attraction in this temperature range and so θ is much lower than in toluene. At

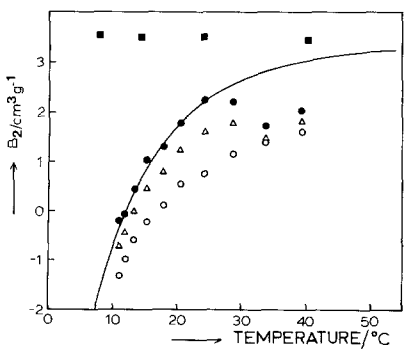

FIG. 7. The second virial coefficient as a function of temperature, ○, $\lambda_0 = 500$ nm; △, $\lambda_0 = 800$ nm, and ●, extrapolated to $\lambda_0^{-2} = 0$ for toluene and ■, extrapolated to $\lambda_0^{-2} = 0$ for *p*-xylene. The drawn line is a theoretical fit of Eq. [6] with $q = 0.8$ cm$^3 \cdot$ g^{-1}, $\Delta = 0.1$ nm, $\sigma = 70$ nm, $L = 22.8$, and $\theta = 353$ K.

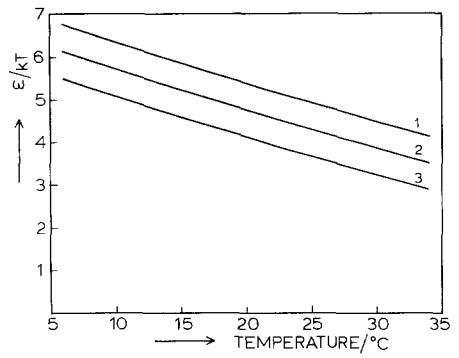

FIG. 8. The depth of the square well (in units kT) at various widths as a function of temperature, as found from a fit of Eq. [6]. (1) $\Delta = 0.05$ nm; (2) $\Delta = 0.1$ nm; and (3) $\Delta = 0.2$ nm.

high temperatures the B_2 of silica in toluene reaches the values measured for *p*-xylene, although there are some irregularities. Thus the hard sphere B_2 does not depend on the type of solvent, in accordance with the model used.

In principle the London–van der Waals forces between the particles cores can be temperature dependent too. The Hamaker constant must then vary considerably with temperature. But since the Hamaker constants for silica in toluene and in xylene (and in benzene also) are about equal one would expect the attractions to develop at almost the same temperature. This is clearly not found experimentally. Moreover increasing the temperature should result in an attraction too, but the dispersion remains stable up to the boiling point (110°C) of toluene.

According to Eq. [11] the $B_{2,app}$ for repulsive interactions (i.e., α is small) must become smaller at decreasing wavelengths. Our experiments do indeed show such a dependence (Fig. 6). For α greater than about 5, Eq. [11] predicts an increase of $B_{2,app}$ at decreasing wavelengths. This however is not found in the experiments, although B_2 goes down to zero and thus α is about 8. The slopes become smaller but they do not change sign at lower temperatures. Of course the range of extrapolation is rather large if one wants to obtain an accurate value of the initial slope. We do not expect a very strong influence of terms higher than K^2 in Eq. [8] since our particles are small.

In the derivation of Eq. [10] it is assumed that the concentration is still low enough for B_2 to account for the nonideality. The experiments were done at relatively high concentrations too and one therefore expects an influence of higher virial terms (Eq. [3]). These effects can be seen in Figs. 4 and 5, where at high concentration the experimental points tend to have larger values than the fitted lines. These higher coefficients possibly change the absolute values of the B_2's, but the variation with temperature will remain. The wavelength dependence is influenced by the higher terms also. The effect of attraction on the values of the higher virial coefficient cannot be accounted for exactly. In a van der Waals-like description [3] these coefficients do not change. If additional experiments are done at higher concentrations it should be possible to obtain the osmotic compressibility in the entire concentration range and find a better equation of state.

It is shown that turbidity can be used to obtain information on the colloidal particles themselves and their interactions in much the same way as with light scattering. Using small particles the turbidity measured is not influenced by multiple scattering. Turbidity measurement is relatively simple, by contrast with light scattering experiments the sample does not need to be filtered to remove dust particles. The apparatus used is an ordinary spectrophotometer with relatively simple cuvettes. A drawback is that turbidity can be measured on strong scattering samples only, but with such samples light scattering cannot be used. Of course one can use very long cuvettes, thus increasing the useful range of the turbidity measurements. Absorption of light must be excluded or accounted for.

In conclusion it should be mentioned that because the interaction can be varied so easily by changing the temperature of the colloidal system such a system will be a very suitable one for studying the properties of attractive

spheres by means of other techniques such as (ultra) centrifugation and rheological measurements. Results of these studies will be reported in future papers.

REFERENCES

1. van Helden, A. K., Jansen, J. W., and Vrij, A., *J. Colloid Interface Sci.* **81,** 354 (1981).
2. van Helden, A. K., and Vrij, A., *J. Colloid Interface Sci.* **78,** 312 (1980).
3. Jansen, J. W., de Kruif, C. G., and Vrij, A., *J. Colloid Interface Sci.* **114,** 471 (1986).
4. Jansen, J. W., de Kruif, C. G., and Vrij, A., *J. Colloid Interface Sci.* **114,** 481 (1986).
5. Dhont, J. K. G., *Physica A* **120,** 238 (1983).
6. van Helden, A. K., and Vrij, A., *J. Colloid Interface Sci.* **76,** 418 (1980).
7. Walstra, P., *Brit. J. Appl. Phys.* **16,** 1187 (1965).
8. Gregory, J., *Adv. Colloid Interface Sci.* **2,** 396 (1969).
9. McQuarrie, D. A., "Statistical Mechanics," p. 235. Harper & Row, New York, 1976.
10. Caljé, A. A., Agterof, W. G. M., and Vrij, A., *in* "Micellization, Solubilization, and Microemulsions" (K. L. Mittal, Ed.), Vol. 2. Plenum, New York, 1977.
11. Brouwer, W. M., Nieuwenhuis, E. A., and Kops-Werkhoven, M. M., *J. Colloid Interface Sci.* **92,** 57 (1983).
12. Bandrup, J., and Immergut, E. H. (Eds.), Polymer Handbook. Wiley, New York, 1975.